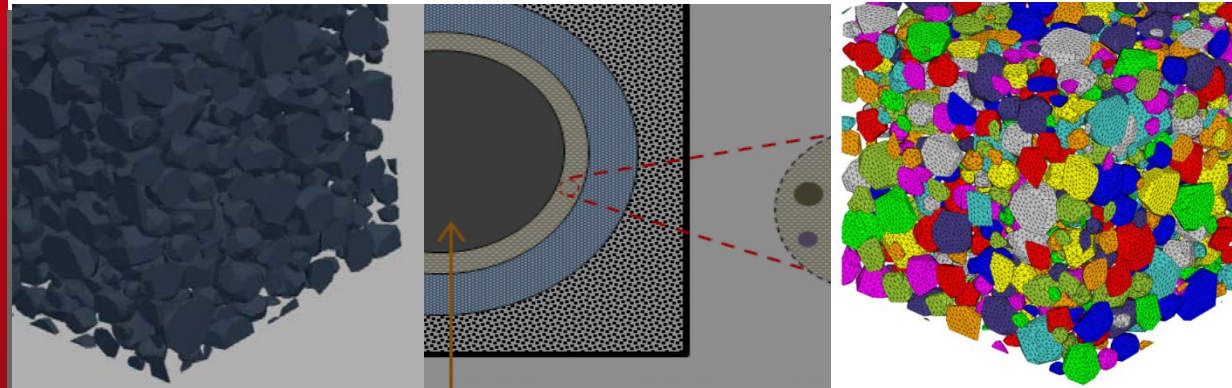


EFFECTIVE AGEING LINEAR VISCOELASTIC PROPERTIES OF COMPOSITES WITH PHASE PRECIPITATION: COMPARISONS BETWEEN NUMERICAL AND ANALYTICAL HOMOGENIZATION APPROACHES



Tulio Honorio^{1,2}; **Benoit Bary**¹ and Julien Sanahuja²

¹CEA, DEN, DPC, SECR, F-91191 Gif-sur-Yvette, France

²EDF MMC (Site des Renardières) 77818 Moret-Sur-Loing Cedex, France

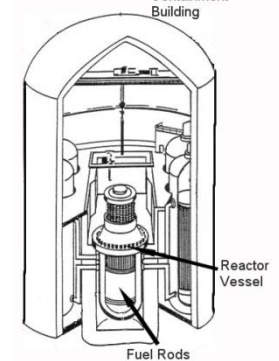
FRAMCOS 9, MAY 29-JUNE 1 2016

Nuclear facilities

Safety and durability of concrete structures are of particular importance

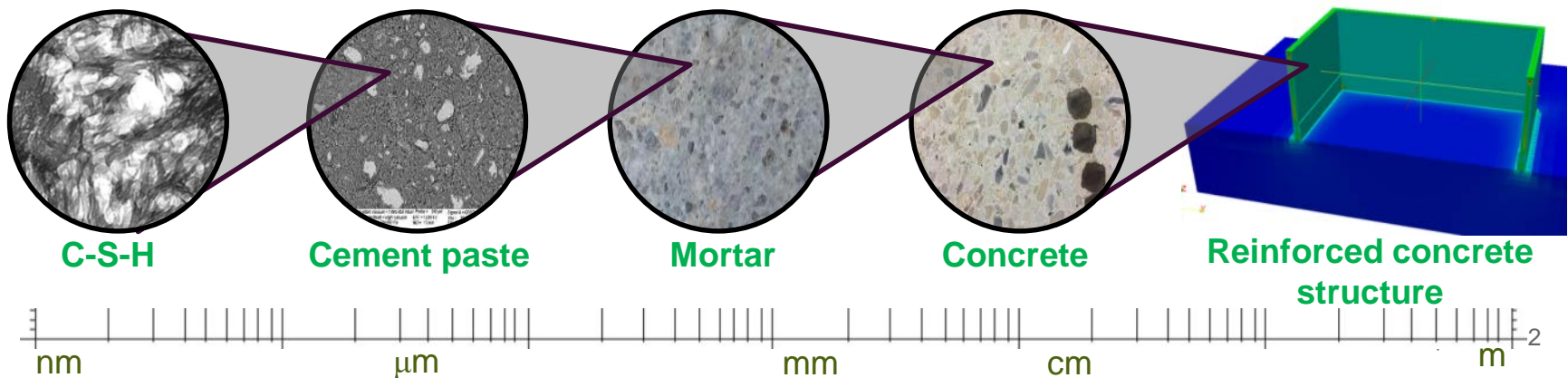
→ **Short as well as long term behavior** when submitted to mechanical, hydric and thermal loadings
 ⇒ **should be precisely characterized**

Nuclear waste storage Confinement building



➔ Focus on the short-term behavior

- Estimation of mechanical properties evolving at early age (hydration)
- Multiscale approach: different phenomena taking place at different time and space scales



Objectives

- Evaluation/validation of a semi-analytical approach for estimating the ageing linear viscoelastic properties of cementitious materials by comparison with 3D numerical simulations

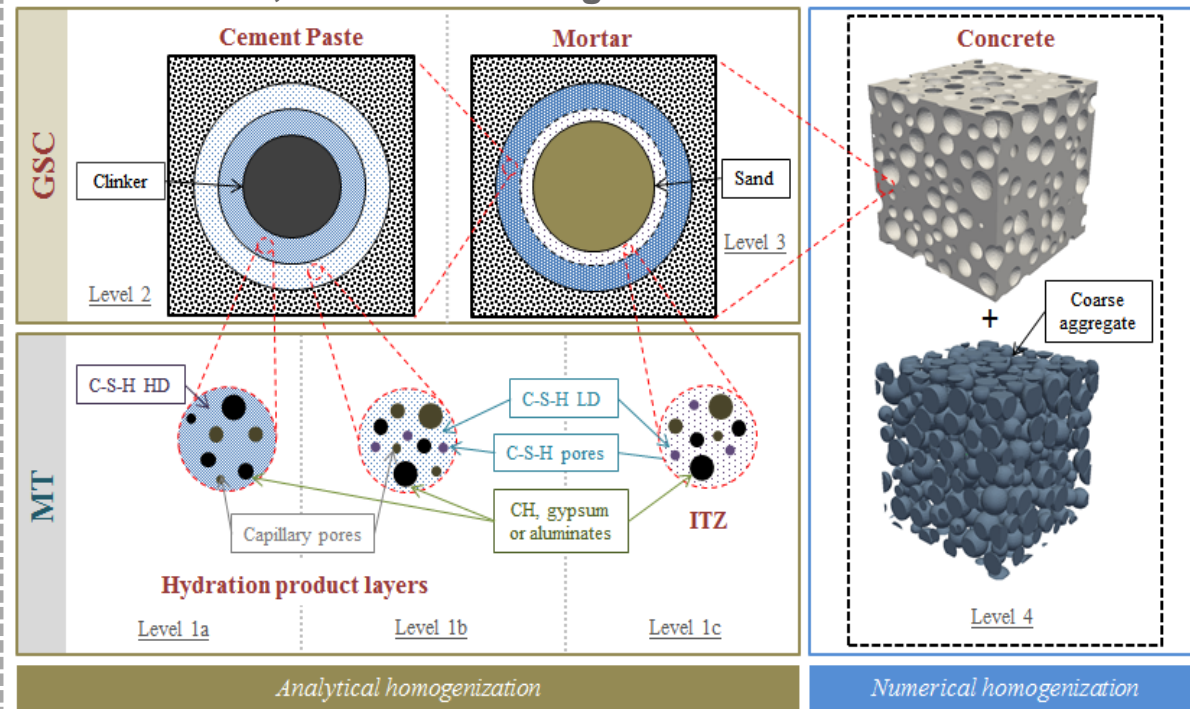
➔ in the case of a progressive precipitation (solidification) scenario

General approach

➔ **Analytical homogenization:**
Estimation of properties at different scales (simplified representation of the microstructure, different phase properties...)

➔ **Numerical homogenization:**
-Validation of analytical approaches
-More complex microstructures
-Analysis of particular aspects: shape of particles, distribution, size...

Example: analytical homogenization at the cement paste and mortar scale, numerical homogenization at concrete scale



- Constitutive behaviour in ageing linear viscoelasticity:

$$\boldsymbol{\varepsilon}(t) = \int_{t'=-\infty}^t \mathbb{S}(t, t') : d\boldsymbol{\sigma}(t') \quad \boldsymbol{\sigma}(t) = \int_{t'=-\infty}^t \mathbb{R}(t, t') : d\boldsymbol{\varepsilon}(t')$$

- Ageing aspect → Dependence of the time of loading

- Non-ageing case $\boldsymbol{\varepsilon}(t) = \int_{t'=-\infty}^t \mathbb{S}(t - t') : d\boldsymbol{\sigma}(t')$ $\boldsymbol{\sigma}(t) = \int_{t'=-\infty}^t \mathbb{R}(t - t') : d\boldsymbol{\varepsilon}(t')$

- Laplace-Carson transform → **Correspondance principle** → equivalence to elasticity
[Mandel1966]

- Volterra integral operator : $(f \circ g)(t, \tau) \equiv \int_{t'=-\infty}^t f(t, t') d_{t'} g(t', \tau)$ [Volterra 1887]

$$\boldsymbol{\varepsilon}(t) = \mathbb{S}(t, \cdot) \overset{\circ}{\hat{=}} \boldsymbol{\sigma}(\cdot), \quad \boldsymbol{\sigma}(t) = \mathbb{R}(t, \cdot) \overset{\circ}{\hat{=}} \boldsymbol{\varepsilon}(\cdot),$$

- Similar form to Elasticity → **Correspondance principle**

- Numerical method to evaluate Volterra integrals: [Sanahuja, 2013]

→ Time discretization + trapezoidal rule [Bazant, 1972]

Derivation of Mori-Tanaka scheme in ageing linear viscoelasticity

- Obtained by [Sanahuja \[2013\]](#)

Derivation of Generalized Self-Consistent scheme (n-layered spherical inclusions)

- Following [Herve and Zaoui \[1992\]](#)

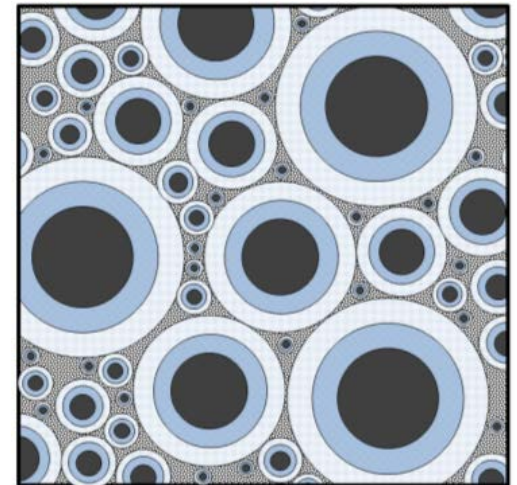
Bulk relaxation function

- For $n = 2$ (1 layer):

$$k_{(2)}^{eff} = \left[R_2^3 k_2 \circ [4\mu_2 + 3k_2]^{-1} \circ [4\mu_2 + 3k_1] - 4\mu_2 \circ [4\mu_2 + 3k_2]^{-1} \circ [R_1^3 (k_2 - k_1)] \right] \circ \left[R_2^3 [4\mu_2 + 3k_2]^{-1} \circ [4\mu_2 + 3k_1] + 3[4\mu_2 + 3k_2]^{-1} \circ [R_1^3 (k_2 - k_1)] \right]^{-1}$$

Shear relaxation function

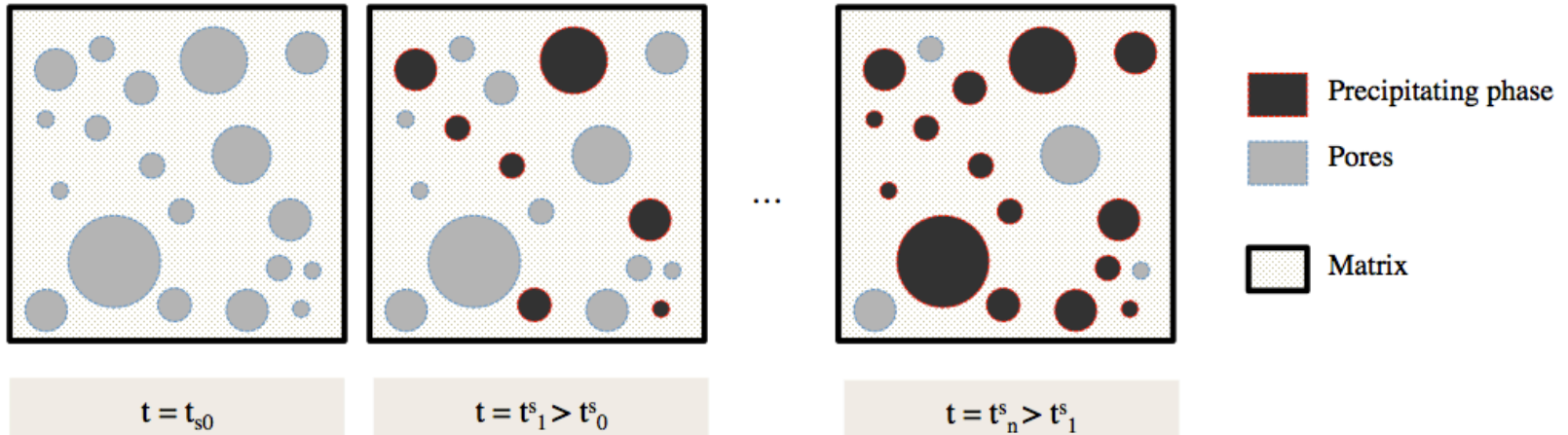
- Problem: Inversion of a matrix with non-commutative elements
 - Schur complement
 - *NCA*lgebra (package for *Mathematica*)



[Honorio et al., under review]

- **Progressive precipitation of phases** → ageing of the material (including in the case of non-ageing behavior of phases [Bazant 1977])

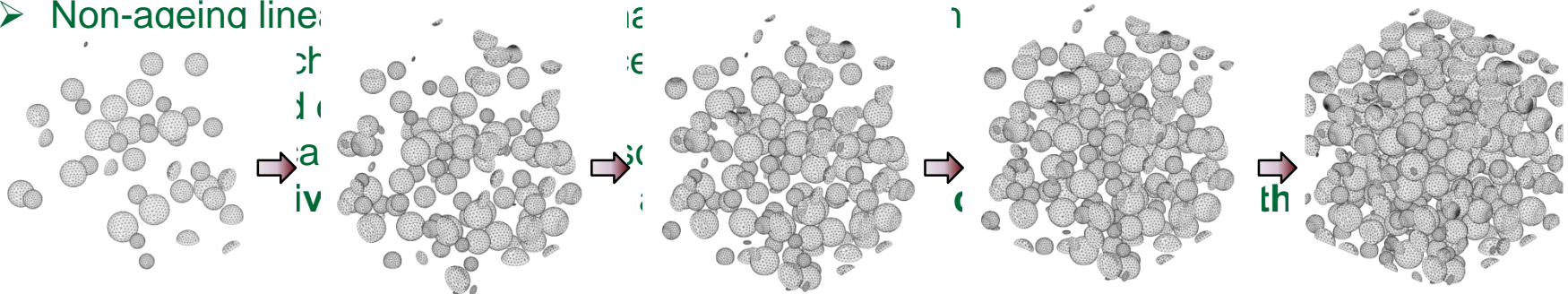
- **Simplified scenario considered in this study:**



Example: precipitation of 30% spherical inclusions

➤ Microstructures = matrix + 1 inclusion phase

➤ Non-ageing line:

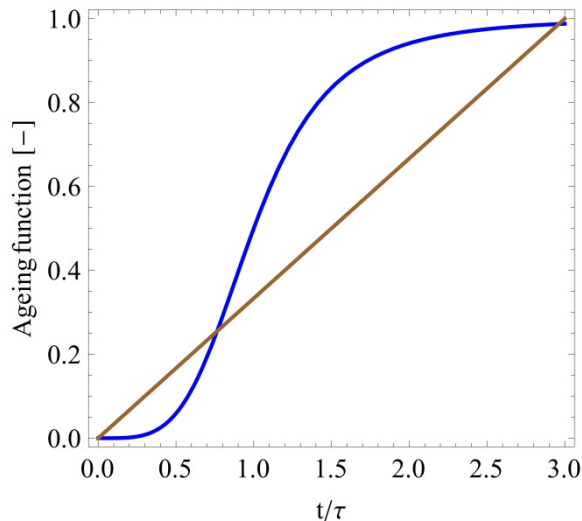


To simplify the comparison → use of idealized behaviors

➤ Two ageing functions are studied:

Linear $f_{age}^B(t) = \min\left(1, \frac{1}{3}t\right) f_{age}^\infty$

Sigmoidal $f_{age}^A(t) = \frac{t^4}{1+t^4} f_{age}^\infty$

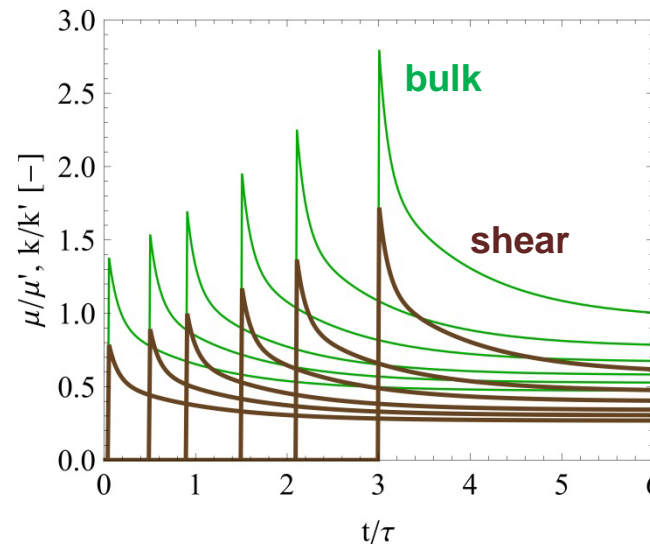


➤ Linear viscoelastic behavior for the phases:
Generalized Maxwell model for bulk and shear moduli

$$\Rightarrow X(t-t') = x_0 + \sum_i x_i \exp[-(t-t')/\chi_i]$$

Parameters

	x_0	x_1	x_2
k/k'	1	1	1
μ/μ'	1/2	1/2	1/2
χ/τ	-	0.1	1



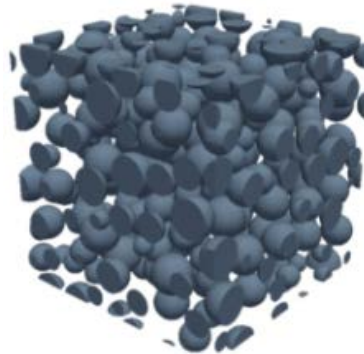
➔ Evolutions of bulk and shear moduli, linear ageing function, 30% inclusions

■ Numerical samples considered → Generation with CAD code salome

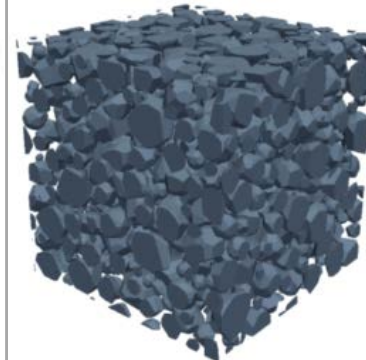
(www.salome-platform.org)

- Randomly distributed inclusions
- Various shapes and sizes
- Periodic meshes

- 360 spherical aggregates of different sizes
- 30%
- $1.75 \cdot 10^6$ finite elements



- 1124 Voronoi aggregates of different sizes
- 40%
- $2.37 \cdot 10^6$ finite elements



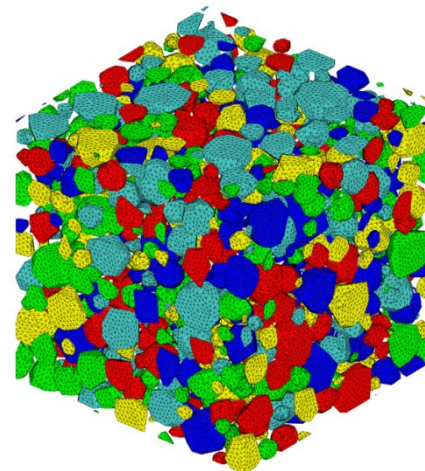
■ Discretization in FE simulations (Cast3M) → random repartition of inclusions

- ➔ Random repartition in a prescribed number of sub-families as a function of the volumes of each aggregate
- ➔ Calculation of the exact precipitation time for each sub-family

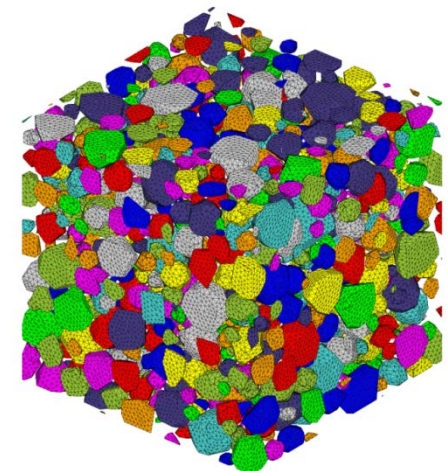
Example : with the 1124 Voronoi aggregates microstructure

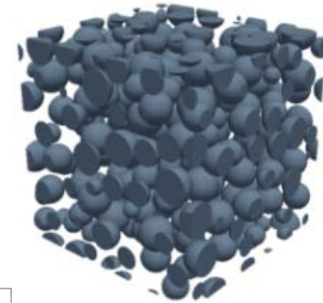


5 sub-families



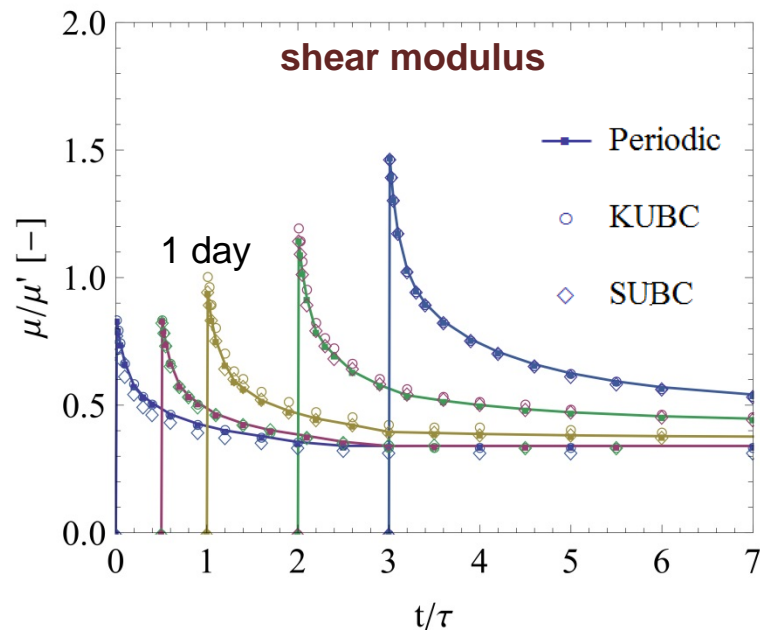
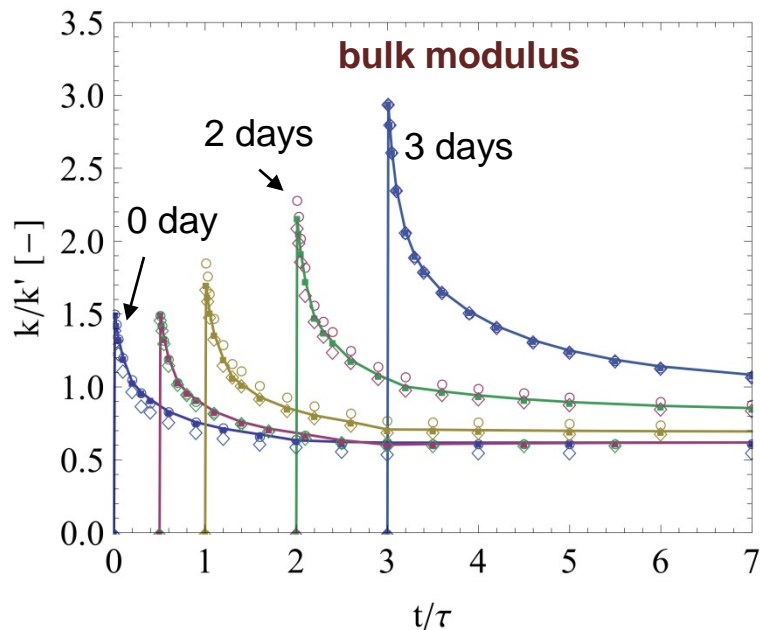
10 sub-families





Numerical simulation results of Representative Element Volumes are known to be dependent on boundary conditions

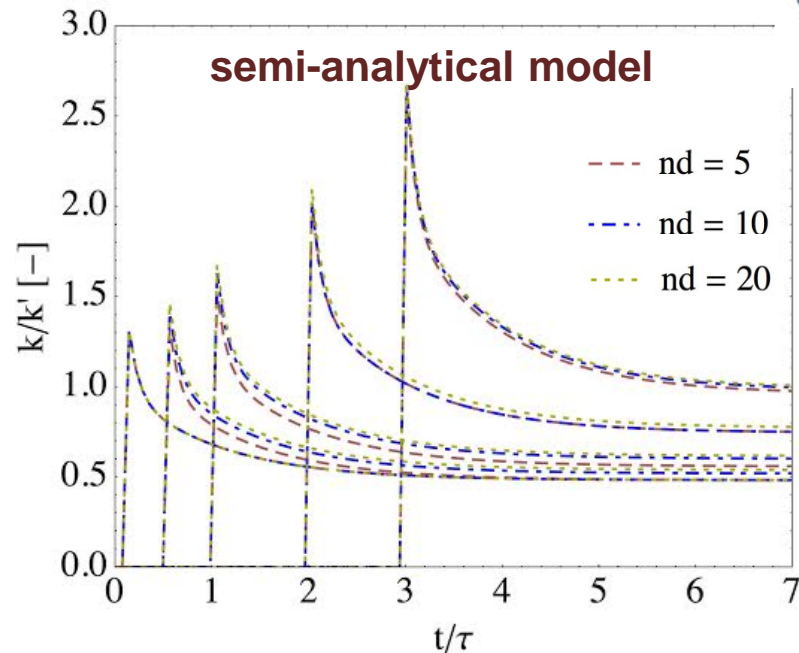
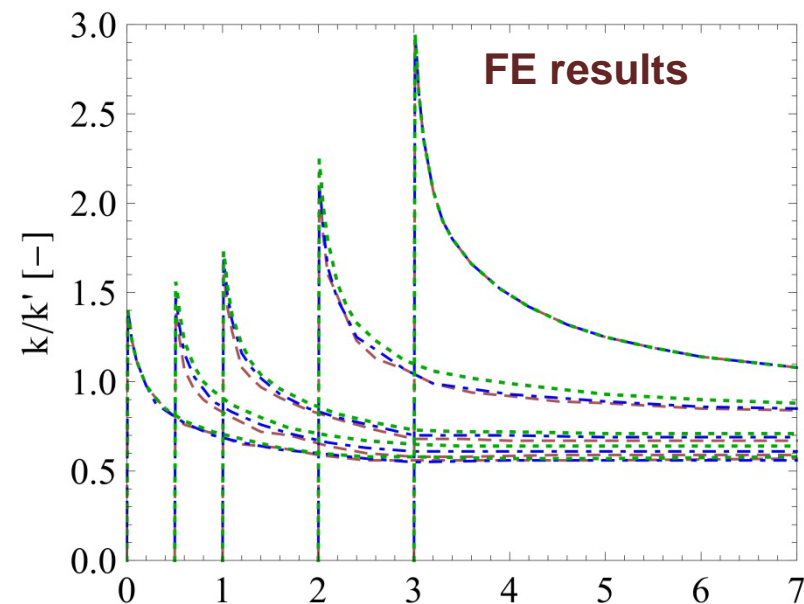
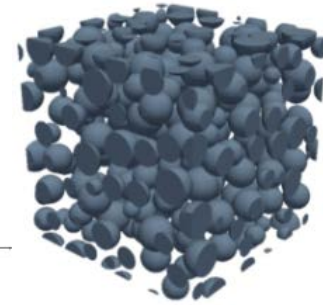
- Linear ageing function
- Age of loading: 0.0, 0.5, 1, 2, 3 days, discretization=10 sub-families
- Boundary conditions considered: static uniform (SUBC), kinematic uniform (KUBC) and periodic (PBC)



- Relatively small differences between the BC
- SUBC close to PBC (taken as reference)
- Computation time with SUBC (1.5-2 hours for 20 time steps) about 2.5 times less than PBC → in the following results are shown with SUBC

■ Discretization to reproduce a progressive precipitation :

- Discretization of the inclusion phase influences both FE and semi-analytical methods
- Example on bulk modulus obtained with 3 discretization levels: 5, 10 and 20 sub-families, 30% spherical inclusion case

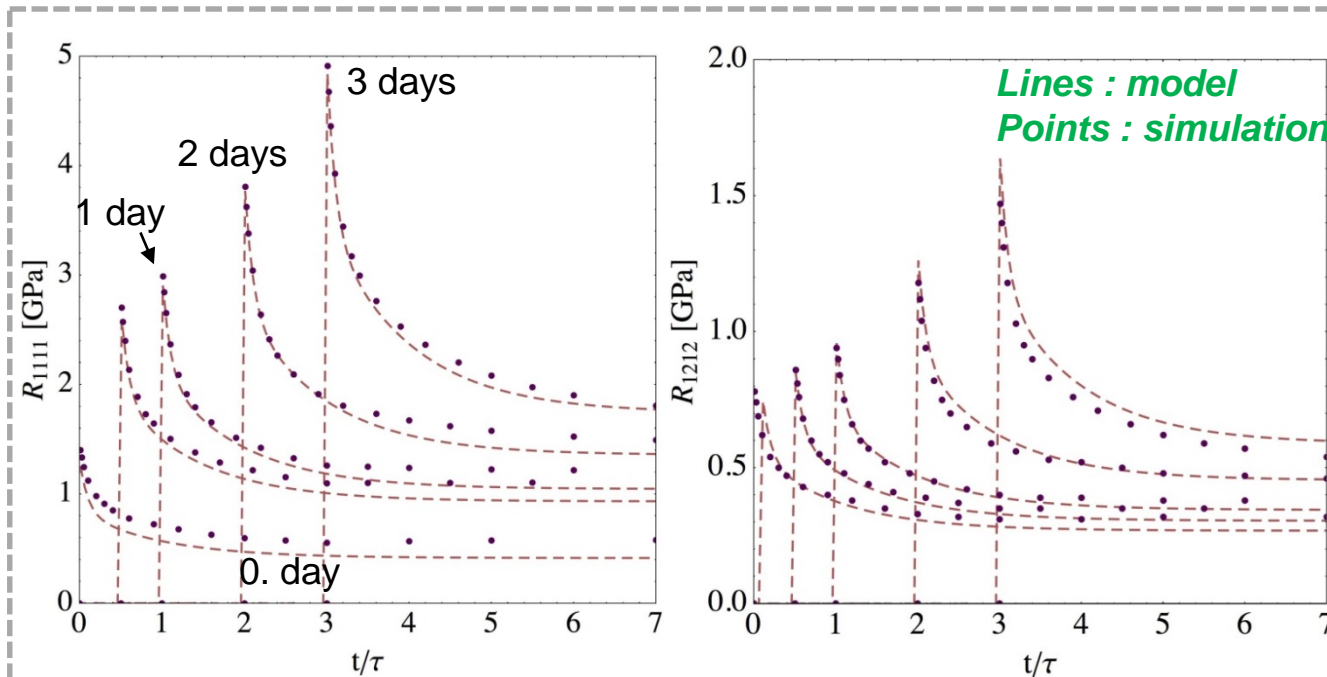
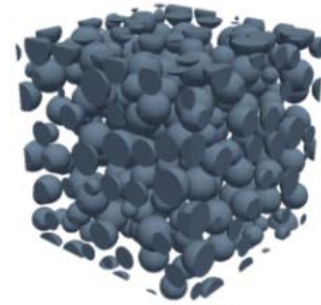


- ➔ Some limited differences are observed as a function of the discretization
- ➔ Discrepancies are of the same order for the FE and model results
- ➔ **At least 10 sub-families for both FE simulations and model**

Relaxation tensor, 30% spherical inclusion case

- Linear ageing function
- Different loading ages: 0.0, 0.5, 1, 2, 3 days

creep



Evolution of the longitudinal stresses in the microstructure



→ Relatively good agreement between FE and semi-analytical results

→ Validation of the analytical procedure

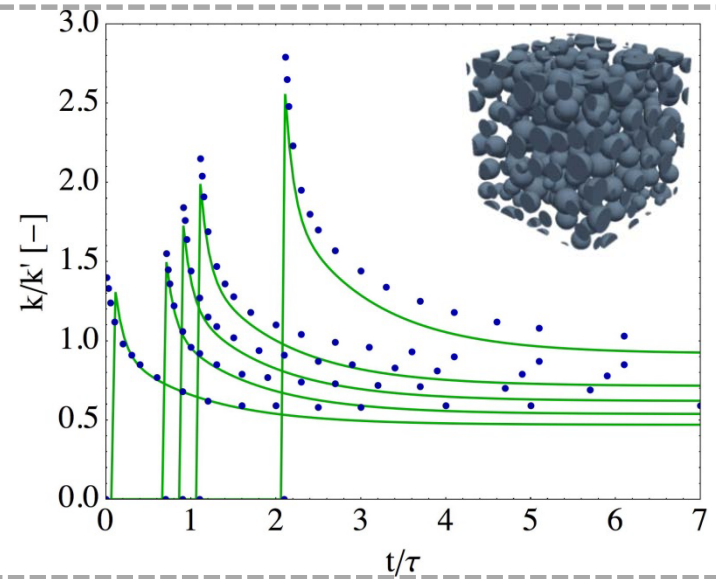
Age of loading: 1 day

Results with sigmoidal ageing function

- 30% spherical inclusions
- Loading times: 0.0, 0.7, 0.9, 1.1, 2 days

→ Relatively good agreement between FE and semi-analytical results of overall moduli

Lines : model
Points : simulation



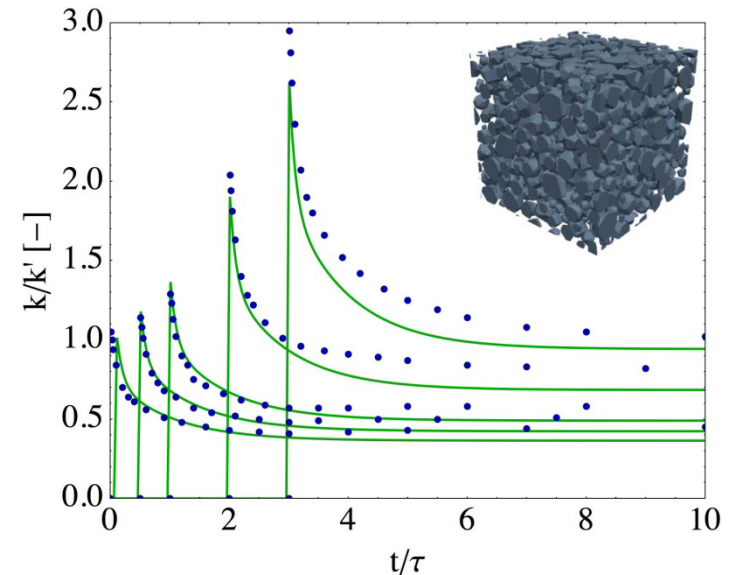
Results with the 40% Voronoi aggregate microstructure

- Linear ageing function
- Different loading times: 0.0, 0.5, 1, 2, 3 days

→ Correct agreement between FE and semi-analytical results, with greater volume fraction of inclusions

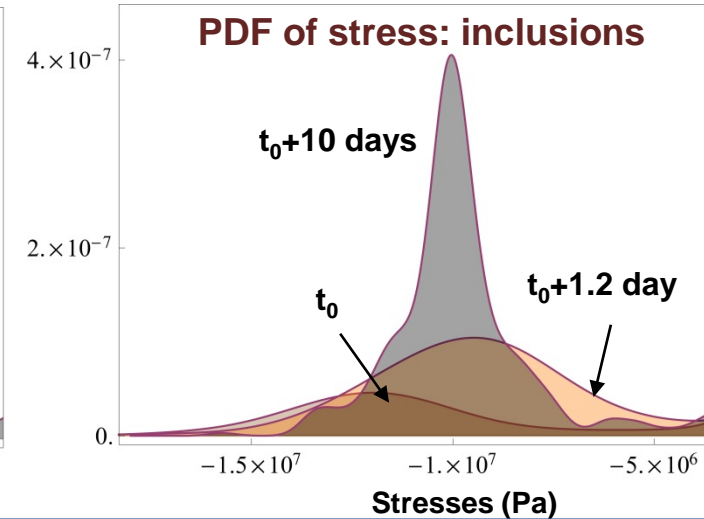
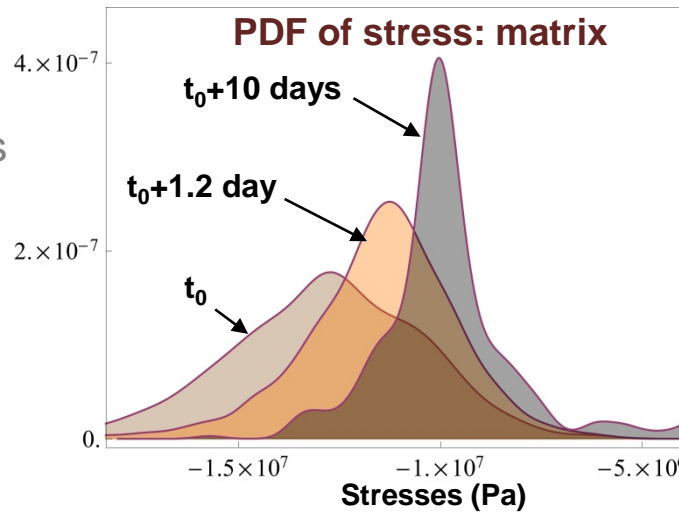
→ Negligible effects of the random discretization process through several realizations (not shown)

→ Effects of the aggregate shape are to be analyzed specifically

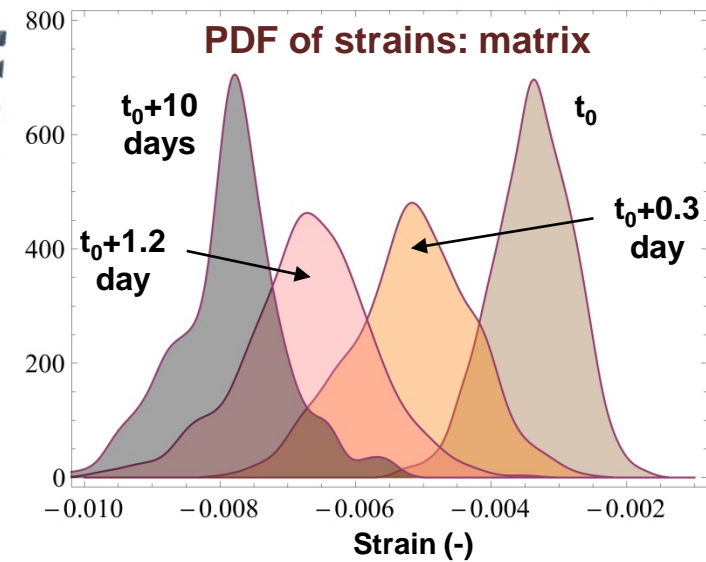
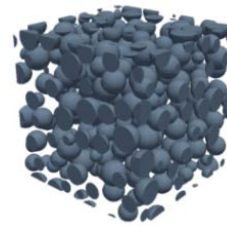


□ Evaluation of the dispersion in the aggregates and matrix

- **Example:** average longitudinal stress and strains within aggregates and matrix subvolumes
- Probability Distribution Functions at different times
- t_0 at loading = 1 day

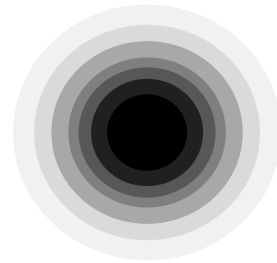
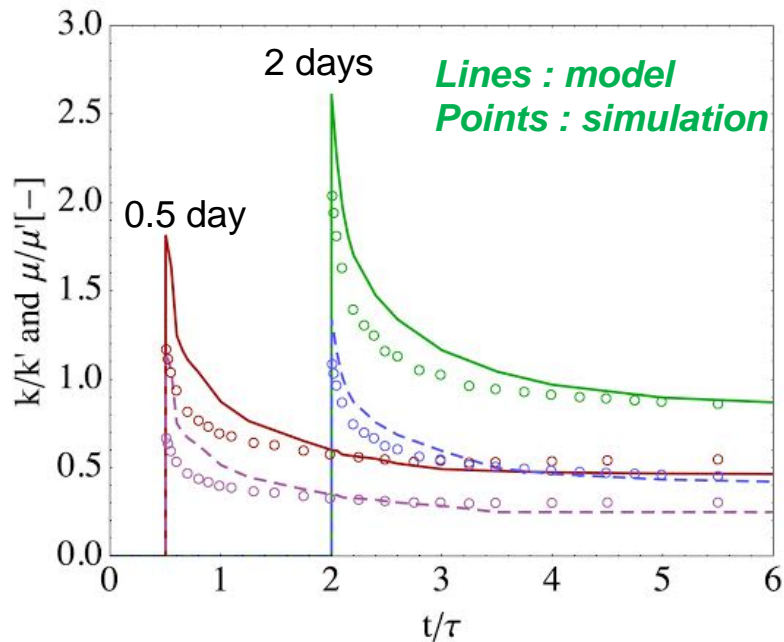


- Large dispersion of stresses in both matrix and inclusion, which decreases for greater times
- Stress distribution appears more disperse in the aggregates than in matrix subvolumes
- Significant dispersion in the matrix strains; the mean strain in the matrix decreases with time

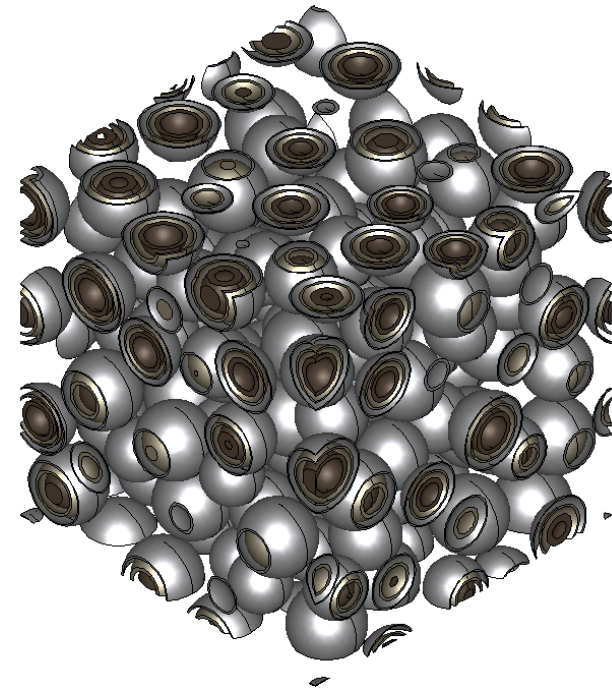


■ First results with 40% multilayer inclusions

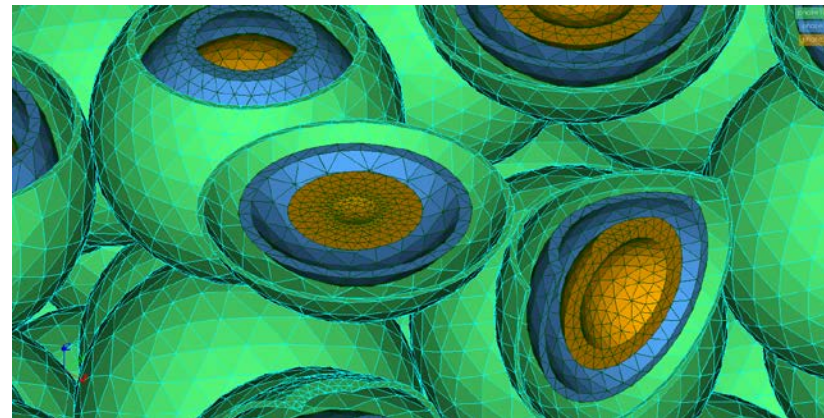
- Progressive precipitation from the external layer to the core
- 120 inclusions composed of 1 core and 9 layers
- 3.57 millions of finite elements
- Use of the GSCS for the analytical estimations



Multilayer inclusion



Details of the mesh



- Correct, but more discrepancies with respect to the MT case
- Aspects to be addressed in the future: effects of the mesh refinement

- 3D FE numerical simulations with scenarios of progressive precipitation of inclusions
- Confrontation with a semi-analytical model for estimating the ageing linear viscoelastic properties of cement-based materials
- The comparison shows generally a correct agreement between FE and analytical results, which validates the analytical procedure

Perspectives:

- Extension and application to the hydration of cement particles
- Introduction of an ageing viscoelastic behaviour of the phases (C-S-H)
- Other precipitation scenarios (multilayer inclusions) to be analyzed
- Extension to other physical properties: coefficient of thermal expansion (in progress)...